J Polym Environ (2018) 26:15–22
DOI 10.1007/s10924-016-0914-0

ORIGINAL PAPER

Water-Blown Castor Oil-Based Polyurethane Foams with Soy Protein as a Reactive Reinforcing Filler

Shuai Zhang[1] · Aimin Xiang[1] · Huafeng Tian[1,2] · A.Varada Rajulu[3]

Published online: 20 December 2016

Abstract To decrease the usage of petroleum based materials, a kind of bio-resource based composite foams were developed with soy protein isolate (SPI) as reactive reinforcing filler in castor oil based polyurethane foams (PUF) prepared by self-rising method using water as a blowing agent. The resulting composite foams were evaluated for their morphology, density, mechanical and biodegradation properties, etc. Fourier transform infrared spectroscopy study exhibited characteristic peaks for SPI and PUF and indicated that the amino groups and hydroxyl groups on SPI reacted with polyphenyl polymethylene polyisocyanates (PAPI) to increase the crosslinking degrees of the composite foams. Densities of the resultant composites were found to increase with increasing SPI content. Mechanical properties of the samples were improved with the increase of SPI content. The compost tests further proved that the composite PUF had better biodegradability than neat PUF. Therefore, this research has provided a simple method of preparing the bio-resource based polyurethane foams, while exploring the potential of using SPI in polyurethane foam applications.

✉ Huafeng Tian
tianhuafeng@th.btbu.edu.cn

[1] School of Materials and Mechanical Engineering, Beijing Technology and Business University, Beijing 100048, People's Republic of China

[2] Key Laboratory for Solid Waste Management and Environment Safety (Tsinghua University), Ministry of Education of China, Beijing 100084, People's Republic of China

[3] Centre for Composite Materials, International Research Centre, Anand Nagar, Krishnankoil 626 126, India

Keywords Polyurethane foam · Soy protein isolate · Mechanical properties · Biodegradability

Introduction

Polyurethane foams (PUFs) are generally produced by the reaction of two chemical feedstocks viz., polyols and isocyanates. Nearly all of these feedstocks are made from petroleum [1, 2]. Global concerns about the depleting petroleum sources and the rising price of petrochemical-derived products have led to investigations into substitutes that are produced from renewable sources and can meet cost and performance requirements of the market [3]. This represents both challenges and opportunities for renewable-based chemicals to supply this billion dollar industry [4]. Due to the limited choice of isocyanates, a majority of the research on renewable substitutes used for the production of PUF has focused on the polyol component. Polyols are alcohols containing two or more hydroxyl functional groups. Currently, most bio-based polyols (biopolyols) are produced from lignocellulosic biomass or vegetable oils [5]. Lignocellulosic feedstocks such as corn stalks, wheat straw, and dried distillers grains have been studied for bio-based polyols [6]. Vegetable oils including castor oil, soybean oil, and palm oil have also been studied as sources of bio-based polyols [7].

The wide range of industrial applications of castor oil has led to a steady increase in demand for this material in the world market [8]. Castor oil is a low-cost, abundantly available, renewable raw material which has attracted research effort because of its potential use in coatings, adhesives, paints, sealants and encapsulating compounds. It can be used as a polyol to develop new and "green" macromolecular architectures. Polyurethanes based on castor oil

with different isocyanates seem to be interesting alternatives to non-renewable based materials in agreement with the concept of sustainable development [9–12].

Utilizing the natural occurring polymers, such as starch [13–17], soy flours (SF) [18], lignin [19] to prepare polyurethane biocomposites or modify their properties and degradability have been published in previous works. These biopolymers possess abundant –OH groups in their polymer chains, so can be utilized as polyol and/or crosslinkers for polyurethane. The incorporation of biopolymers into polyurethane foams can not only improve the biodegradability but also reduce the cost of the resulting foams. Soy protein, as a byproduct of soy oil industry, is a polymer containing amino acids which can be converted to biodegradable plastics through extrusion with plasticizer [20–22]. Compared with soy flour and soy protein concentrate (SPC), soy protein isolate (SPI) possessed a higher protein content of more than 90% and was usually used as the pure soy protein to prepare soy protein based biomaterials. The potential uses of soy plastics as biodegradable commodity products such as spoons, toys and food packaging are reported [23–25]. However, the potential application of soy protein plastics is limited because of its low strength and high moisture absorption. There are many researches on the study and modification of soy protein based resin for fabricating plastics, including blending [26], chemical modification [27, 28], reinforceing [29], etc. For example, biodegradable plastics by blending soy protein with polyester amide or poly (butylene adipate-co-terephthalate) (PBAT) possess fine mechanical properties and low water sensitivity [30].

In this work, environment-friendly composite foams from SPI and castor oil based PUF were developed and it was expected to fabricate the bio-resource based composite foams which would decrease the usage of petroleum based materials. The influence of SPI content on the structures and properties of castor oil based foams was investigated. The foams are intended to find applications as packaging, external insulation, sound insulating materials, etc.

Materials and Methods

Materials

Castor oil, trolamine, dibutyltindilaurate were purchased from Sinopharm Chemical Reagent Company, China. Surfactant (AK-8805) was donated by Jiangsu Maysta Chemical Co., Ltd, China. Polyphenyl polymethylene polyisocyanates (PM-200) was purchased by Wanhua Chemical Group Co., Ltd, China. Soy protein isolate (SPI) was purchased by HuBei Yu Long Soybean Protein Co., Ltd, China. (Yumeng, China). The dry protein content of SPI used was more than 90%.

Preparation of Polyurethane Foams

Calculated amounts of castor oil, catalyst (1.5% of polyol), surfactant (3% of polyol), water (2% of polyol), and SPI (0, 5, 10, 15 and 20% of polyol) were premixed thoroughly with a mechanical stirrer for 30 s. To this mixture, an appropriate amount of PAPI was added to give an isocyanate index of 1.40 and stirred at 2000 rpm for 10–15 s. The mixture was then poured immediately into a $25\times25\times5$ cm^3 mold and was allowed to free foaming at room temperature. The resulting foam was removed from the mold after 1 hour and was allowed to cure at room temperature for one week before testing.

Characterization

Fourier transform infrared (FTIR) spectra of the foams were recorded by KBr pellet method using Nicolet iN10 MX device (Thermo Fisher Scientific, US). The FTIR measurements were performed in the 4000–400 cm^{-1} range at 4 cm^{-1} resolution.

The cell morphology of PUF was observed using a scanning electron microscope (SEM, JSM-5800). The samples were gold-coated before scanning to provide an electrically conductive surface. The average cellular diameter of the PUF was statistically analyzed by Image-Pro Plus software.

Closed cell ratio was obtained according to ASTM D6226-2010 on UltraPYC 1200e (Quantachrome, US) and calculated from Boyle's Law. A known volume was pressurized in the Quantachrome chamber and the pressure change was correlated to the actual volume, thus allowing the closed cell ratio of the sample to be calculated. Three specimens of each composition had been tested and the average values were reported.

The apparent density of the PUF samples was determined according to ISO 845:2006. The size of the specimen was $25\times25\times25$ mm (length × width × thickness). The apparent densities of three specimens per sample were determined and the average values are reported. The compression strength was measured on a testing machine (MTS systems China Co, Ltd) according to ISO 844-1787. The size of the specimen was $50\times50\times20$ mm (length × width × thickness), and the rate of crosshead movement was fixed at 2.0 mm/min for each sample. The compression direction of the foam is parallel to the growth of the foam. The relative deformation is 10%. Average values of five specimens per sample are reported.

The biodegradation behaviors of the foams were determined in terms of composting. The foams were cut into slices with thickness of about 3 mm, and then buried in

soil. The samples (1.0 g) were mixed with 72 g of soil, 24 g of top soil, 8 g of mature compost, and 50 g of water in 250 mL glass beaker. The beaker was kept in an oven controlled at the desired temperature (30 °C). The soil composition and compost conditions resembled those described in ASTM D 5988-03. After a given time, the samples were taken out of the container, washed thoroughly, and dried in vacuum. The change in cellular structure of the foam was observed using SEM and the structure changes were characterized by FTIR.

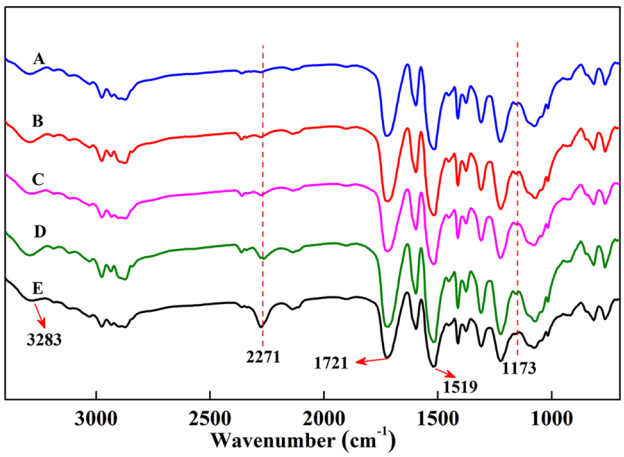

Fig. 1 The FTIR spectra of PUFs prepared with different SPI contents

Results and Discussion

Evidence for SPI Participation in PUFs Formation

In order to study whether SPI participated in the reaction with PAPI or just acted as a physical filler in the foam, FTIR analysis of the obtained PUFs was carried and the spectra are shown in Fig. 1. Five different samples for FTIR analysis were prepared: A: PUF with 20 wt% SPI, B: PUF with 15 wt% SPI, C: PUF with 10 wt% SPI, D: PUF with 5 wt% SPI and E: control-PUF without SPI. The structure of the polyurethane was confirmed by the presence of the main absorption bands characteristicof urethane moieties: 3275 cm^{-1} (N–H), 1721 cm^{-1} (C=O urethane), and 1519 cm^{-1} (N–H amide II groups). Three distinct characters were observed. First, the peak at 2271 cm^{-1} appeared in the spectrum of sample E and assigned to free isocyanate (–NCO) groups, was barely seen in the spectra of samples A, B and C. Given that the component ratio of sample A, B and C are the same, it clearly indicates that extra -NCO groups were consumed by SPI. Secondly, a new absorption peak around 1173 cm^{-1} appeared only in the spectra of sample A, B, C and D, which was attributed to the carbonyl stretch of urea functionality (–HNCONH–). This indicates that the amino groups and hydroxyl groups on SPI reacted with PAPI, as illustrated in Fig. 2. Abundant reactive groups on the SPI chains could react with –NCO groups. Therefore, introduction of SPI is expected to improve the degree of crosslinking of the system. Thirdly, the peak of the N–H gradually shifted from 3275 to 3292 cm^{-1}. The

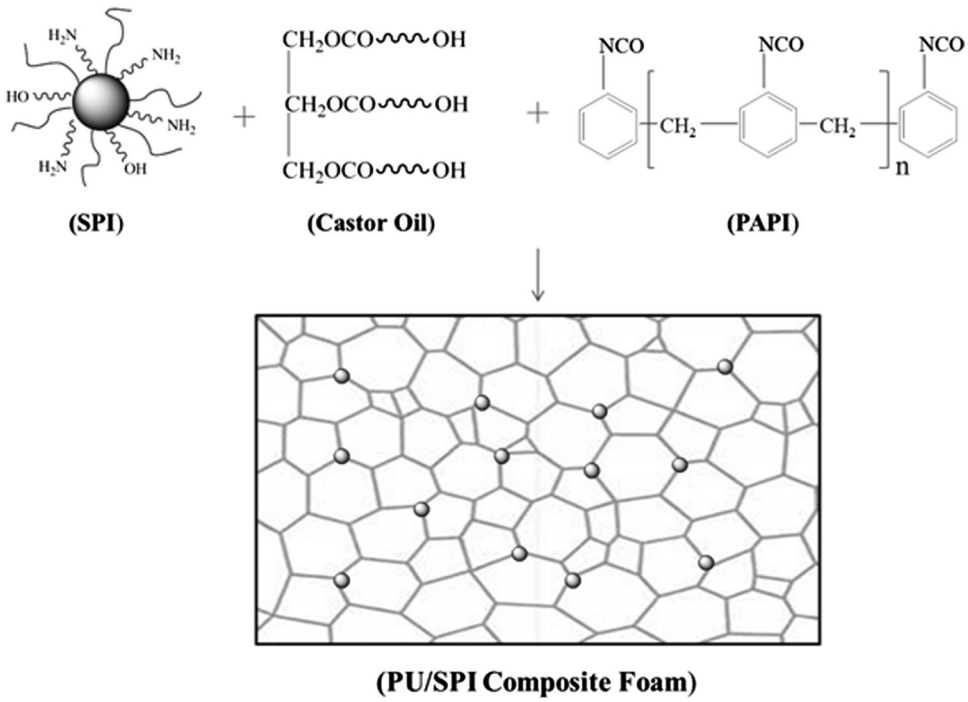

Fig. 2 The schematic representation of the reaction between SPI and PAPI

shift to a higher wavenumber suggests that the incorporation of SPI disturbed the hydrogen bonding between N–H and C=O and improved the microphase separation between hard and soft segments due to the strong interaction between SPI and polyurethane molecules. As a conclusion, SPI at least partially participated as a reactant in the synthesis of PUFs.

Foam Morphology

Figure 3 shows the SEM images of PUFs in presence of different SPI content. From the micrographs, it is evident that the PUFs had polygon closed-cell structure. As observed from the micrograph of the neat PUF (Fig. 3a), the cell size and cell distribution were nearly uniform. For SPI reinforced PUFs, no obvious phase separation was observed for all the compositions. The chemical reactions discussed above could provide strong interactions between SPI filler and PU matrix, resulting in fine compatibility between them. With the addition of SPI, the overall cell structure became more uniform, the cell walls became thinner and the amount of closed cells increased. Alteration in the cell morphology was mainly due to the presence of SPI particles that can act as gas nucleation sites during the foaming process.

The average cellular diameter of the PUFs was statistically analyzed by means of Image-Pro Plus software from SEM images, and the average values are summarized in Fig. 4. It is evident that the neat foam had fewer cells with a larger cell size than other composite foams. In other words, the composite foams had higher number of cells with a smaller cell size as the amount of SPI increased. Composite foams with 5, 10, 15 and 20 wt% SPI had a

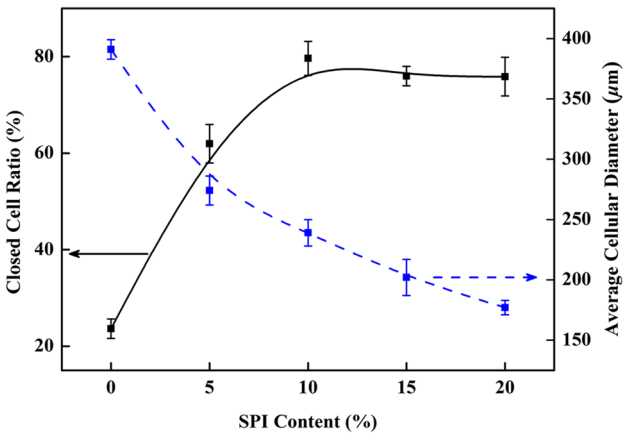

Fig. 4 The average cell diameter and closed cell ratio of PUFs with different SPI contents

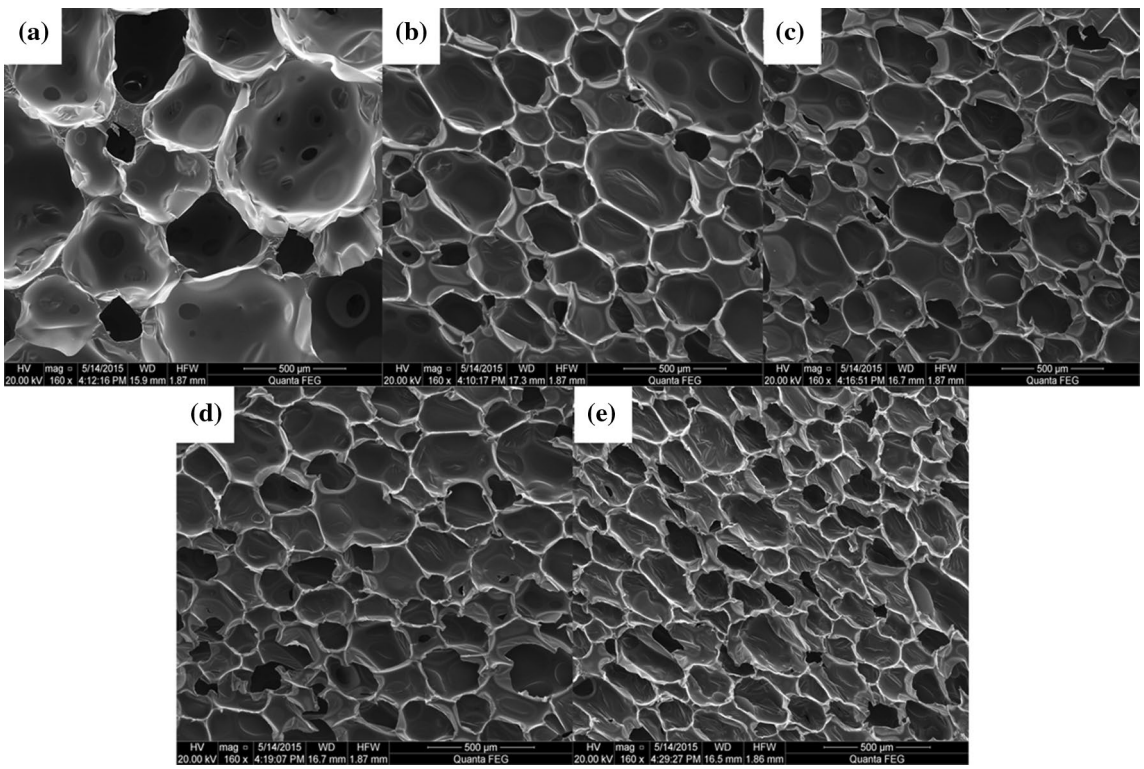

Fig. 3 SEM images of cell structure of PUFs in presence of different SPI contents—**a** 0 wt%, **b** 5 wt%, **c** 10 wt%, **d** 15 wt% and **e** 20 wt%

cell size of 274, 239, 202 and 177 μm, respectively, compared with 391 μm of neat PUF. This indicates that the composite foams containing SPI had a higher cell density and smaller cell size than those of the neat foam. So, it can be concluded that the SPI had an effect on reducing the cell size. This may be due to the increased viscosity of the system after SPI addition which restrained the expansion of the cells.

The closed cell ratio of foam composites is shown in Fig. 4. With the increase of SPI content, closed cell ratio increased rapidly and reached a plateau when the SPI content was more than 10 wt%. Due to the presence of reinforcing effect as well as the crosslinking effect of the SPI, foam cell walls are expected to get higher strength. During foaming and curing process, the gas in cells was unable to break through the cell walls, resulting in the increase of closed cell ratio. However, under the closed cell ratio growing situation, the average cellular diameter continues to decrease. There would be a stronger inner gas pressure in smaller cells, which makes the gas inside the cells a higher possibility to break through the cell walls, leading to higher opening ratio. Integrating the two factors, it can be inferred that for high content of SPI, the closed cell ratio of the foams reached a plateau.

Density and Mechanical Properties

Rigid foams need to have a density higher than 30 kg/m^3 to keep adequate strength to bear certain load for commercial applications, such as pipe insulation and refrigerator insulation. The density of the plastic foam is determined by the weight and volume of the plastics matrix and the gas trapped in the foam cells.

The density and compression strength of PUFs containing SPI at different weight percentage are shown in Fig. 5. The density and compression strength of the foams increased with increasing SPI content. Neat PUF possessed the lowest density of 63 kg/m^3 and the lowest compression strength of 0.17 MPa. While the samples with 20 wt% SPI possessed the maximum density of 91 kg/cm^3 and the highest compression strength of 0.24 MPa. The phenomenon may be explained from the following aspects. First, the polyurethane foams in this study were prepared by chemical foaming with CO_2 as the foaming agents produced by water and isocyanate reaction. As SPI and isocyanate reaction does not increase the CO_2 volume, the solid phase composition increases with increasing SPI content leading to an increase in the foam density. Further, mechanical properties of the foam are mainly associated with the density. Thus, the compression strength increased with the increase of density of PUFs. Secondly, this phenomenon is also attributed to the high modulus of soy protein in dry state and could exhibit reinforcing effect in polymer matrix [31].

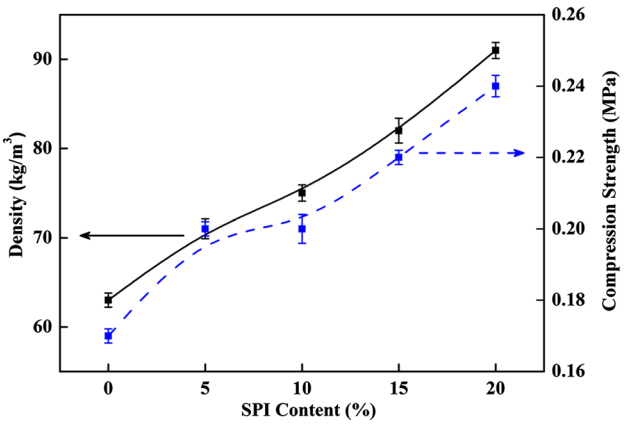

Fig. 5 Effect of SPI content on the density and compression strength of PUFs

Besides this, the higher compression strength might also be due to the higher crosslink density and stronger cell walls after SPI incorporation as compared to control foams. The fine closed cell structures also contributed the improved mechanical properties. Therefore, the density and strength would meet the requirement of applications such as building heat insulating, sound absorption, packaging, etc. with the demand of density and strength more than 35 kg/m^3 and 0.18 MPa, respectively, which would possess wide application potentials in these areas.

Thermal Properties

Thermal properties of foams were analyzed by TGA and the thermograms are shown in Fig. 6. The decomposition of the neat polyurethane foams occurred in three stages: dissociation of the unstable urethane bond at a temperature between 150 and 330 °C, decomposition of the soft polyol segments at a temperature between 330 and 400 °C, and the further degradation of the fragments generated after the second stage. All the foams exhibited more or less weight loss below 150 °C, due mainly to the volatilization of additives and water. In the first stage, all the composite foams showed better thermal stability than neat foams and foams composite with 15 wt% SPI showed the best thermal stability, due to high crosslink density. Because the PUF service temperature usually does not exceed the upper limit of the first stage temperature, SPI incorporation can be considered beneficial to the application of foam. In the other two stages, the foam pyrolysis behaviors were irregular. The lower weight loss of composite foams during the second half was due to the more number of fragments generated after the decomposition of the soft polyol segments. DTG curves corresponding to neat PUF reveal three maximum peaks suggesting at least three main degradation processes (Fig. 6b). The similar trend was observed for the composite

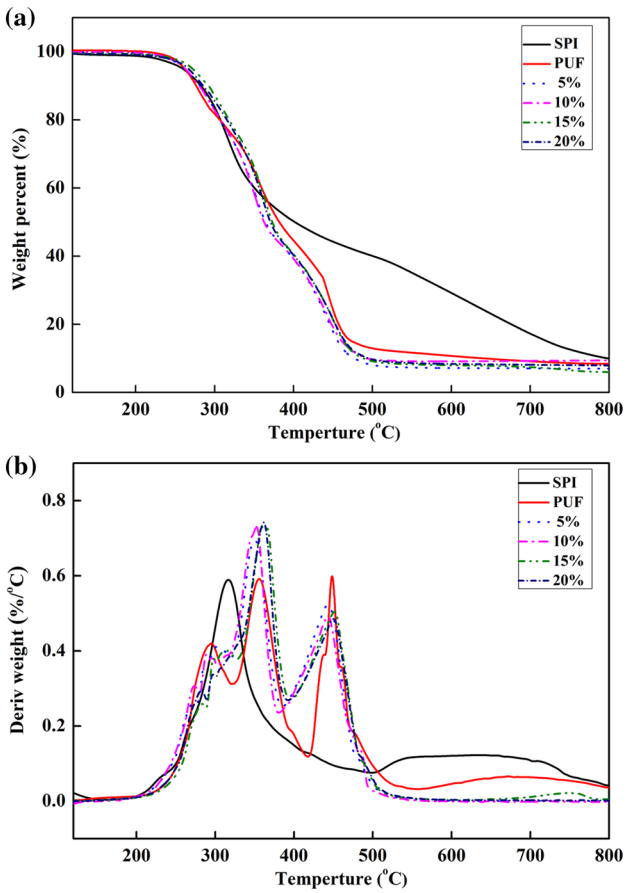

Fig. 6 **a** TGA and **b** DTG curves of PUFs made with different SPI contents

with 5, 10, 15 and 20 wt% SPI. From these results, we conclude that SPI did not influence the basic mechanisms of the thermal degradation of the PUFs but on the other hand improved the thermal stability of the composites.

Biodegradation Behaviors

The biodegradability of the PUFs samples was investigated by composting. Photographs of PUFs with different SPI content before and after composting are shown in Fig. 7. The morphology of the neat foam was smooth before biodegradation, and no major change such as cracking or piercing could be detected on the surface after one month's or three months' biodegradation except the color change of the surface, indicating a low degradation rate. When SPI was introduced, the surface of PUFs was covered by the microbes. SEM images of PUFs before and after composting are shown in Fig. 8. For neat PUF sample (Fig. 8b) after composting, the original cell structures can still be identified, and just appeared a little erosion after 3 months' biodegradation. In contrast, for the composite foam with 20 wt% SPI, the cell structures were destroyed and the remaining became a loose network after serious biodegradation. The cell frame was totally destroyed. This is due to the fact that SPI itself was biodegradable. Further, SPI provides nutrient which was conducive to microbial attachment and growth on the foam surface as well as the formation of microbial community, resulting in the accelerated degradation of composite foam. From this observation and comparison with neat foam, one may conclude that SPI accelerated the degradation rate of PUFs.

FTIR spectroscopy was further used to analyze structural changes of PUFs before and after 3 months of composting (Fig. 9). Characteristic bands of urethane bonds in the neat PUFs were located at 1720 and 1521 cm^{-1}. No substantial decrease was observed in the intensity except for the 1720 cm^{-1} band. Decrease in the carbonyl (C=O) bond could be related to the ester segments of the foams. Further analysis revealed that bands assigned to the ester C–O bond (1226 cm^{-1}) also showed significant decreases in intensity after composting (Fig. 9a). These results suggest that the ester bonds of glyceride and or frame structures were preferred sites of attack for biodegradation of castor oil-based PUFs during composting. Other studies on the biodegradation of PUs made from bio-based polyols, including castor oil polyol [32] and soybean oil polyol [33], have also reported that these glyceride based ester linkages are susceptible to microbial attack.

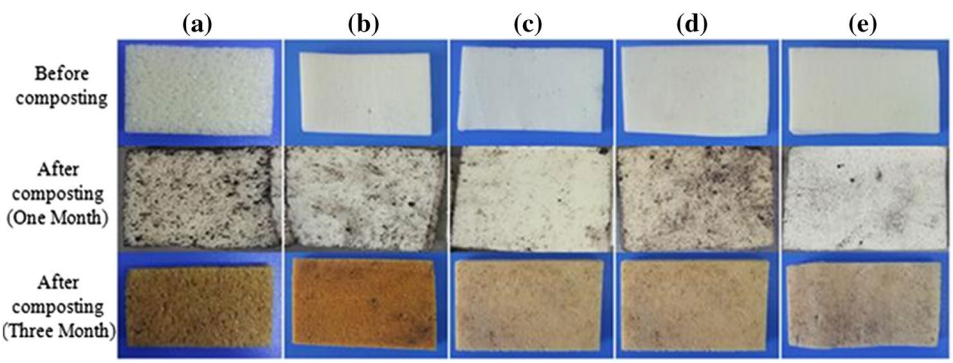

Fig. 7 Photographs of PUFs before and after composting. SPI content: **a** 0 wt%, **b** 5 wt%, **c** 10 wt%, **d** 15 wt% and **e** 20 wt%

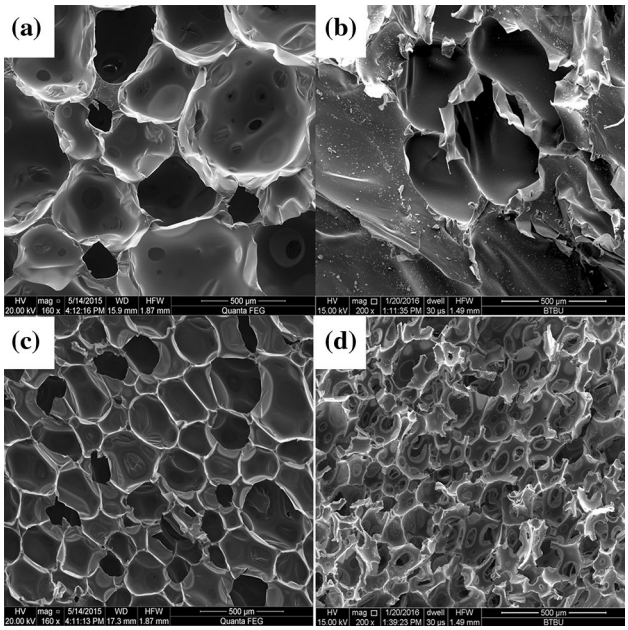

Fig. 8 SEM images of neat foam (**a** before, **b** after) and composite foam with 20 wt% SPI(**c** before, **d** after) before and after 3 months of composting

The FTIR spectra of the composite foams are shown in Fig. 9b. Only marginal decrease in the intensity of the bands assigned to the urethane segments at 1508 (N–H) and 1306 cm^{-1} (urethane C–O) vibrations were observed. Obvious decrease was observed in the intensity of the bands associated with the ester segments at 1716 cm^{-1} (C=O) and 1233 cm^{-1} (C–O) stretching vibrations. These results indicated that ester segments in the composite foams were preferred by microbial attack, whereas little degradation occurred in the urethane linkages.

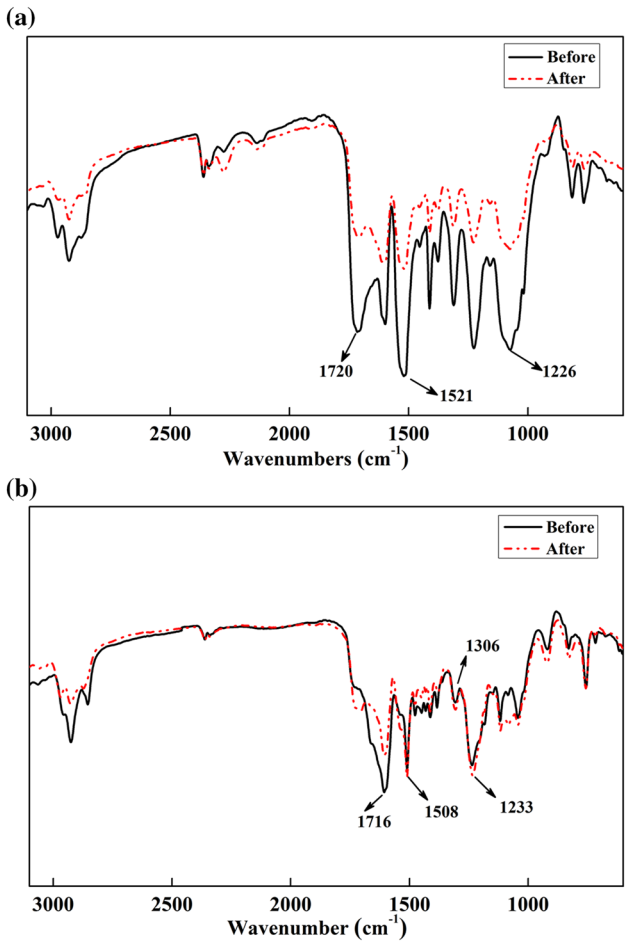

Fig. 9 FTIR spectra of **a** neat foam and **b** composite foam with 20 wt% SPI before and after 3 months of composting

Conclusions

A series of PUFs with different SPI content were successfully synthesized. The amino groups and hydroxyl groups on SPI could react with PAPI, leading to improved degree of crosslinking of the system. All the composite foams maintained a regular cell structure and had even smaller average cell size and higher closed cell ratio than the neat PU foams. The composite foam with SPI showed higher compression strength and density. Composite foam with 20 wt% SPI showed better compression strength (0.24 MPa), higher closed cell ratio (76%) and increased by 41.2 and 230.4% as compared to the neat foam, respectively. The most prominent structural changes occurred in the composite foam and the cell frame was totally destroyed during composting, indicating fine biodegradation performance. SPI increased the degradation rate of PUFs. FTIR analysis indicated that the ester segments (C–O and C=O) were preferred sites of attack for the degradation of PUFs. Considering the worldwide abundance of soy protein, composite foams with SPI may become more environmental-friendly substitute for conventional disposable packaging polyurethane foams.

Acknowledgements This work was supported by the National Natural Science Foundation of China (51373004 and 51203004), Beijing Top Young Innovative Talents Program (2014000026833ZK13), Open Funding of Key Laboratory for Solid Waste Management and Environment Safety (Tsinghua University), Ministry of Education of China (SWMES 2015-02).

References

1. Gupta RK, Ionescu M, Radojcic D, Wan X, Petrovic ZS (2014) Novel renewable polyols based on limonene for rigid polyurethane foams. J Environ Polym Degr 22(3):304–309

2. Desroches M, Escouvois M, Auvergne R, Caillol S, Boutevin B (2012) From vegetable oils to polyurethanes: synthetic routes to polyols and main industrial products. Polym Rev 52(1):38–79
3. Babb DA (2012) Polyurethanes from renewable resources. Advances in polymer. Science 245:315–360
4. [4] Duan J, Reddy K O, Ashok B, Cai J, Zhang L, Rajulu A V (2016) Effects of spent tea leaf powder on the properties and functions of cellulose green composite films. J Environ Chem Eng 4(1):440–448
5. Li Y (2011) Development of polyurethane foam and its potential within the biofuels market. Biofuels 2(4):357–359
6. Xu J, Jiang J, Hse C, Shupe TF (2012) Renewable chemical feedstocks from integrated liquefaction processing of lignocellulosic materials using microwave energy. Green Chem 14(10):2821–2830
7. Campanella A, Bonnaillie LM, Wool RP (2009) Polyurethane foams from soy oil-based polyols. J Appl Polym Sci 112(4):2567–2578
8. Moghadam PN, Yarmohamadi M, Hasanzadeh R, Nuri S (2016) Preparation of polyurethane wood adhesives by polyols for mulated with polyester polyols based on castor oil. Int J Adhes Adhes 68:273–282
9. Mutlu H, MeierM AR (2010) Castor oil as a renewable resource for the chemical industry. Eur J Lipid Sci Technol 112(1):10–30
10. Cordero AI, Amalvy JI, Fortunati E, Kenny JM, Chiacchiarelli LM (2015) The role of nanocrystalline cellulose on the microstructure of foamed castor-oil polyurethane nanocomposites. Carbohydr Polym 134:110–118
11. Zhang L, Zhang M, Zhou Y, Hu L (2013) The study of mechanical behavior and flame retardancy of castor oil phosphate-based rigid polyurethane foam composites containing expanded graphite and triethyl phosphate. Polym Degrad Stab 98(12):2784–2794
12. Luo Z, Shi Y, Zhao D, He M (2011) Synthesis of epoxidatied castor oil and its effect on the properties of waterborne polyurethane. Proced Eng 18:37–42
13. Alfani R, Iannace S, Nicolais L (1998) Synthesis and characterization of starch-based polyurethane foams. J Appl Polym Sci 68(5):739–745
14. Yoshioka M, Nishio Y, Saito D, Ohashi H, Hashimoto M, Shiraishi N (2013) Synthesis of biopolyols by mild oxypropylation of liquefied starch and its application to polyurethane rigid foams. J Appl Polym Sci 130(1):622–630
15. Barikani M, Mohammadi M (2007) Synthesis and characterization of starch-modified polyurethane. Carbohydr Polym 68(4):773–780
16. Kwon OJ, Yang SR, Kim DH, Park JS (2007) Characterization of polyurethane foam prepared by using starch as polyol. J Appl Polym Sci 103(3):1544–1553
17. Kim DH, Kwon OJ, Yang SR, Park, J S, Chun BC (2007) Structural, thermal, and mechanical properties of polyurethane foams prepared with starch as the main component of polyols. Fibers Polym 8(2):155–162
18. Chang LC, Xue Y, Hsieh FH (2001) Dynamic-mechanical study of water-blown rigid polyurethane foams with and without soy flour. J Appl Polym Sci 81(8):2027–2035
19. Luo X, Mohanty A, Misra M (2013) Lignin as a reactive reinforcing filler for water-blown rigid biofoam composites from soy oil-based polyurethane. Ind Crops Prod 47:13–19
20. Dash S, Swain S K (2013) Effect of nanoboron nitride on the physical and chemical properties of soy protein. Compos Sci Technol 84:39–43
21. Friesen K, Chang C, Nickerson M (2015) Incorporation of phenolic compounds, rutin and epicatechin, into soy protein isolate films: mechanical, barrier and cross-linking properties. Food Chem 172:18–23
22. Koshy RR, Mary SK, Thomas S, Pothan LA (2015) Environment friendly green composites based on soy protein isolate-A review. Food Hydrocoll 50:174–192
23. Routray M, Rout SN, Mohanty GC, Nayak PL (2013) Preparation and characterization of soy protein isolate films processed by compression and casting. J Chem Pharm Res 5(11):752–761
24. Silva SS, Oliveira JM, Benesch J, Caridade SG, Mano JF, Reis RR (2013) Hybrid biodegradable membranes of silane-treated chitosan/soy protein for biomedical applications. J Bioact Compat Polym 28(4):385–397
25. Tian H, Wu W, Guo G, Gaolun, B, Jia Q, Xiang A (2012) Microstructure and properties of glycerol plasticized soy protein plastics containing castor oil. J Food Eng 109(3):496–500
26. Ji J, Li B, Zhong WH (2011) An ultraelastic poly (ethylene oxide)/soy protein film with fully amorphous structure. Macromolecules 45(1):602–606
27. Fang QH, Zhou D, Han WC, Gao Y, Wang N, Yang F (2012) Preparation of soy protein isolate modified by glutaric dialdehyde and its application in rubber composite. Key Eng Mater Trans Tech Publ 501:208–214
28. Kumar R, Zhang L (2009) Soy protein films with the hydrophobic surface created through non-covalent interactions. Ind Crops Prod 29(2): 485–494.
29. Guo G, Zhang C, Du Z, Zou W, Li H (2015) Structure and properties of poly (vinyl alcohol)/soy protein isolate blend film fabricated through melt processing. J Environ Polym Degr 23(2):183–189
30. Guo G, Zhang C, Du Z, Zou W, Tian H, Xiang A, Li H (2015) Structure and property of biodegradable soy protein isolate/PBAT blends. Ind Crops Prod 74:731–736
31. Jong L (2015) Influence of protein hydrolysis on the mechanical properties of natural rubber composites reinforced with soy protein particles. Ind Crops Prod 65:102–109
32. Wang HJ, Rong MZ, Zhang MQ, Hu J, Chen HW, Czigany T (2008) Biodegradable foam plastics based on castor oil. Biomacromolecules 9(2):615–623
33. Shogren RL, Petrovic Z, Liu Z, Erhan SZ (2004) Biodegradation behavior of some vegetable oil-based polymers. J Environ Polym Degr 12(3):173–178